

163-17204

Code 1

GENERAL MILLS ELECTRONICS GROUP
Aerospace Research Department
2003 East Hennepin Avenue
Minneapolis 13, Minnesota

SPUTTERING EFFECTS
ON THE MOON'S SURFACE

Third Quarterly Status Report
Contract NASw-424

UNPUBLISHED PRELIMINARY DATA

Covering Period 18 October 1962 - 17 January 1963

Submitted to:

National Aeronautics and Space Administration
Office of Grants and Research Contracts
Washington 25, D.C.

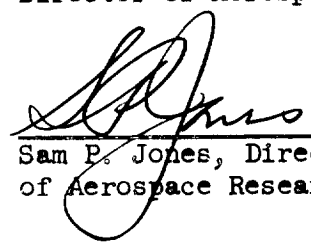
Prepared by:

G. K. Wehner

Submitted by:


G. K. Wehner, Assistant
Director of Aerospace Research

Approved by:


Sam P. Jones, Director
of Aerospace Research

Report No. 2364
Date: 30 January 1963
Project: 89278

TABLE of CONTENTS

	Abstract	iii
I.	Introduction	1
II.	Sputtering Yield of Terrestrial Rocks	1
III.	Sputtering Yield Measurements with Mass Separated Hydrogen Beams	
	A. Introduction	2
	B. Apparatus	6
	C. Results	8
IV.	Sputtering Yields at the Lunar Surface	11
V.	Lunar Surface Structure	13
VI.	Personnel	22
VII.	References	23
	Illustrations	19, 20, 21

ABSTRACT

17204

Sputtering yields of various terrestrial rocks under Hg^+ -ion bombardment of several hundred ev energy were determined with a high frequency sputtering method. Yields by volume are found to be in the same range as that of Fe, a medium sputtering rate metal.

Sputtering yields of metals and oxides were determined with a method where mass separated hydrogen beams (H^+ , H_2^+ , and H_3^+) at ~ 7 kev sputter holes into thin target foils. The method and results are described in detail. Results show that chemical reactions of the hydrogen with the target material may have a decisive influence on sputtering yields. For quartz, one finds a yield of 0.019 for H_2^+ and 0.034 for H_3^+ at 7.5 kev.

Recent literature data on the solar wind, especially from Mariner II, and our new experimental sputtering yields are incorporated in a revised table on lunar sputtering rates. According to this, the moon loses about 0.4 g/year and must have lost in 4.5×10^9 years roughly a 17-cm thick layer.

Ion-bombarded powder samples produce a surface which has photometric properties which are very similar to those required from moon surface studies. The dust particles become cemented together and form a fibrous crust with needles and deep small holes and a slag-like appearance. Oxides are reduced and the surface becomes enriched with metal atoms.

SPUTTERING EFFECTS ON THE MOON'S SURFACE

Third Quarterly Status Report

I. INTRODUCTION

Laboratory experiments were continued with sputtering yield measurements of various rocks under Hg^+ -ion bombardment and with mass separated hydrogen beams.

Recent literature on solar wind flux, velocity, and composition data, in particular, results from measurements with the Mariner Venus probe, together with our new yield results were incorporated in a revised table on sputtering yields at the lunar surface. The surface configuration and structure of the lunar material as found from photometric studies of the moon is discussed in relation to our experimental results on ion-bombarded dust samples.

II. SPUTTERING YIELDS OF TERRESTRIAL ROCKS

Sputtering yields relative to Fe of several igneous rocks were determined by utilizing the high-frequency techniques described in the Second Quarterly Status Report. Target rings were cut from chunks by use of an ultrasonic impact grinder. All samples were baked at $300^{\circ}C$ in air for one hour before sputtering to remove moisture introduced with the impact grinder slurry. The following are the average sputtering weight ratios obtained for these rocks when sputtered under Hg^+ -ion bombardment at ion energies of several hundred ev.

<u>Material*</u>	<u>Sputtered Weight Ratio to Fe</u>
Basalt	0.45
Rhyolite	0.33
Jaspelite	0.50
Volcanic Glass	0.30
Gabbro	0.40
Syenite	0.60

The surface of the rhyolite was darkened and some dark-grey metallic inclusions in the jaspelite were reduced to form a bright metallic surface. Microscopic examination revealed etching of the surface for all materials sputtered.

Although in these experiments neither the ion nor the ion energy directly simulate the solar wind conditions, one can at least conclude that the sputtering yields of these rocks are, by volume, of the same order as that of Fe. Experiments in hydrogen and helium plasmas will be the next important step for obtaining more pertinent data on this important question.

III. SPUTTERING YIELD MEASUREMENTS WITH MASS SEPARATED HYDROGEN BEAMS

A. Introduction

To evaluate sputtering of surfaces by atoms of the solar wind, one needs data on the sputtering yields for the ions H^+ and He^{++} on metals and metal oxides with incident energies in the range 1 to 10 kev. One expects identical sputtering yields for He^{++} and He^+ ions having the same velocity. O'Briain, Lindner, and Moore¹ obtained yields for 9.25 kev

* Rocks courtesy of Dr. L. Cooper, Hamline University, St. Paul, Minnesota.

H^+ , H_2^+ , and D^+ ions on Ag by employing a radioactive tracer technique. Grönlund and Moore² extended this work on Ag to include yield curves from 2 to 12 kev for the ions H^+ , H_2^+ , H_3^+ , D_1^+ , D_2^+ , D_3^+ , and He^+ . By employing a large mass separator (calutron), Yonts, Normand, and Harrison³ were able to obtain sufficiently large ion currents to study the sputtering of Cu by a weight-loss technique. For D^+ ions, they found a decreasing yield from 10 to 40 kev. The deeply penetrating H^+ ions actually caused an increase in the target mass through self-burial. Recently, we⁴ reported yields for 18 metals under bombardment by 7 kev H_2^+ and H_3^+ ions. Our technique employs the mass-analyzed beam to drill a hole in a thin foil.⁵

The results of these studies show that the yields for hydrogen and helium ions are 10^{-2} to 10^{-3} of those for more massive ions like Ne^+ or Ar^+ at the same energy. Therefore, it is imperative that mass analysis of the ions be performed to remove the small number of (heavier) impurity atoms. Besides, in the case of hydrogen, the protons are accompanied by the molecular ions H_2^+ and H_3^+ in amounts that are sensitive functions of source parameters such as pressure, geometry, current, and voltage. However, it is clear that the mass analysis can be very crude and the deflection of the ions in a magnetic sector field through an angle of about 30° or less is sufficient for obtaining reliable results.

Whatever the technique employed, a difficulty is posed by the low yields, which are typically 10^{-2} atoms/ion. Thus, a target having molecular weight 100 loses only 37 micrograms per milliamper-hour of bombardment. Neutron activation of metals having convenient isotopes is a very

sensitive method for measuring small amounts of sputtered material, but it is limited to certain metals. Sensitive microbalances can be employed within a vacuum system⁶ to monitor small weight changes. In either case, one is led to larger ion currents to achieve greater numbers of sputtered atoms in a fixed time so one uses, in general, a fairly large apparatus.

In contrast, the hole-drilling method favors use of a small apparatus. One measures the average area density D of a foil, directs a beam of known energy onto the foil, and monitors the current to the foil and to a collector placed behind the foil at the place where the sputtered hole appears. It is possible to eliminate the influence of secondary γ -electrons and of space-charge-compensating electrons within the beam in the measurement of the ion current. The experiment is terminated when the hole approaches the beam size. This is indicated by a leveling off of the currents to the collector and to the target foil. From the area A of the hole and the integral Q of the ion current that strikes the area A , one computes the yield Y in atoms/ion from $Y = KA/Q$, where $K = DF/M$ is characteristic of the foil, F is the Faraday constant, M is the atomic weight of the foil. For a given beam on a given metal, it follows that (yield \times current density \times time) is a constant. One therefore maximizes the current density (not current) by miniaturizing the apparatus. At the same time, one is free to choose A as small as is practicable so as to reduce the power dissipated in the foil.

The hole-drilling method bypasses the objection of buried hydrogen that is inherent in a weight-loss technique. The surface where the beam is focused is being cleaned by sputtering, but the yield is obtained from the area of

greatest current density only. Yonts and Harrison⁷ have shown that sputtering yields begin to be reduced when the influx of reactive gas atoms to a surface exceeds the flux of sputtered atoms from the surface, i.e., when a full monolayer of gas atoms can be maintained on the surface despite the sputtering. It is often observed that a darkening of the target foils occurs at the fringes of the beam, though it is never seen at the hole edge; the high sputtering rate there seems to overcome the formation of surface layers such as might arise from cracking oil molecules on the surface. Such surface layers would reduce the measured yield for either a weight-loss or a radioactive tracer technique.

The hole-drilling technique might result in yields systematically too large due to individual crystallites being etched free and falling from the foil (incomplete sputtering). The effect appears to be negligible, since discontinuous rises in the current to the collector would be visible.

Obtaining yields for metallic oxides by the hole-drilling technique is especially favorable relative to the weight-loss or radioactive tracer techniques because no difficulties arise for determining the ion beam current. One measures simply the current that passes through the foil to the collector. It is also desirable to measure the current to the foil to be sure that the ion current is constant. In the case of the anodized foils, adequate conduction is obtained through the oxide film. To measure the current to oxide foils, we evaporate a thin film of Ag on the foil. If the film of Ag faces the beam, it is rendered thermally

incoherent in a time short by comparison to the time necessary to sputter through the Ag film. The foil then heats up above the Ag melting point and evaporates the remaining Ag. Satisfactory results are obtained with the Ag film facing away from the beam. In view of the small thickness of the foil (10-30 μ) large electric field strengths for modest charging of the foil surface ensures adequate electrical conductivity through the hot foil.

As indicated above, the heat dissipation through the metal oxide foil would be formidable, but the Ag film also solves this problem. An approximate solution for the temperature rise of a foil of thickness t at the edge of a beam ($A = \pi r_0^2$) delivering P watts of power, assuming cylindrical symmetry, is $T(r) = (P/2\pi kt) \ln (r/r_0)$ where k is the thermal conductivity of the foil and r is the distance to the clamp at the reference temperature. In our apparatus, r/r_0 is about 10 but the magnitude of T/P depends only logarithmically (insensitively) upon that ratio. Thus, for a typical metal foil 25 μ thick, the temperature rise per watt is of the order of 100°C. On a metal oxide, 1 μ of Ag per watt is adequate to cool the insulator below the Ag melting point (961°C).

B. Apparatus

The details of the apparatus are given in our annual AEC report "Surface Bombardment Studies".⁴ In brief, ions are extracted from a Uniplasmatron source in a Pierce gun geometry such that space-charge limited currents form a rectilinear beam in the extraction gap. Then

a converging lens partially overcomes the divergent effect of the break in the electric field at the extraction electrode aperture and of the space-charge within the beam, so that a nearly parallel beam passes through the jaws of a permanent magnet inside the bell jar. The beams of H_2^+ and H_3^+ strike a target assembly with two Faraday cups behind a foil that is 4 mm x 10 mm. The two beam centers are separated by 2.4 mm at 7 kev with the foil at the edge of the magnet gap. For an extraction hole diameter of 0.4 mm, optimum focus produces an etched ellipse on the target foil 1.0 mm in major diameter and a hole in the foil 0.3 mm in major diameter, depending upon termination time. Current densities of 100 ma/cm² are obtained, but this density can readily be reduced by defocusing the beam and turning down the plasma current. Proton current is too low for sputtering a hole in any but the materials of highest yield.

The background pressure in the source is 5×10^{-6} torr; the pressure must be lower than this in the bell jar which is pumped with an impedance an order of magnitude lower. The source is operated at the desired power level for eight hours before the accelerating voltages are applied and the run is started so that thermal equilibrium (and hence mechanical stability) can be obtained and so that source and bell jar will be degassed. At this point, the source pressure will drop to its base value if the hydrogen leak is valved off and the filament turned down. If the filament is left hot, the Ta heat shields will emit occluded hydrogen for a long time.

C. Results

The results for 18 metals which we collected under AEC sponsorship⁴ are presented for reference in Table I and Fig. 1. Included in Table I are the yields Y_2 and Y_3 for H_2^+ and H_3^+ ions at the stated energies plus the ratio $R \equiv Y_3/Y_2$ together with the estimated standard deviations in these quantities arising from uncertainties in measuring A, Q, and D. Table I shows, furthermore, our first results on the sputtering rate of oxides by hydrogen ions, giving the yields for Al and Ta foils that were each anodized to an oxide film 0.30- μ thick on each surface.

The Ta and Al foils that were anodized may be assumed otherwise identical to the pure metal foils. In the case of Ta, 0.6 μ of oxide in a 17- μ thick foil does not seem to significantly change the yield from that of the pure metal. If the oxide sputtering yield would be one order of magnitude lower than that of Ta, the 0.6 μ of oxide would be equivalent to 6 μ of extra metal. With at least 10% precision in this hole-drilling technique, such a 30% effect would be readily detectable. On the other hand, the yield for anodized Al is significantly reduced by an amount that does indicate that the yield for Al_2O_3 is about an order of magnitude lower.

Quartz was blown into large bubbles and fragments were flat enough to be clamped in the target assembly without cracking. Often the beams produced sufficient additional thermal strain to crack the foils, however. From eight runs on quartz we present the following results:

<u>kv</u>	<u>Y₂ (molecules/ion)</u>	<u>Y₃ (molecules/ion)</u>	<u>Comments</u>
7.5	0.019	0.034	20% uncertain, 2 days sputtering time
8.3	No sputtering	0.014	20% uncertain, 4 days, currents as above

The uncertainties arise principally in the interpretation of the current records. The latter result is included to demonstrate the effect of an air leak in the bell jar that raised the reactive gas pressure at the foil by an unknown amount.

On the basis of these preliminary results, we suggest that the chemical activity of hydrogen is important in the sputtering of oxides. Most stopped and neutralized hydrogen ions will be in the form of H_1^0 in the lattice. Atomic hydrogen is placed higher than Al but lower than Mg in the electromotive force series. Since Ta at room temperature is placed between Pt and Au in the electromotive force series, it is not surprising that its oxide is readily reduced and the "oxide" surface sputters as a pure metal. Similarly SiO_2 is probably reduced to Si metal. But apparently even the active atomic hydrogen does not compete favorably with the very electropositive Al for oxygen bonds in the lattice--even if those bonds are disturbed by the near passage of another stopping proton.

Implicit in this picture of reduction of the oxide is the assumption that oxygen is pumped away in the form of H_2O more rapidly than it is impinging from the residual gases. The latter influx in obvious notation is

$$j_0 = \frac{1}{4} P N_0 \sqrt{\frac{8}{\pi MRT}}$$

which for air at 300°K and 2×10^{-6} torr amounts to 7.5×10^{14} molecules/cm²/sec. For the 7.5-kev run on SiO₂ the average ion current densities were $j_2 = 0.90$ ma/cm² and $j_3 = 0.70$ ma/cm². The latter value is equal to 4.4×10^{15} H₃⁺/cm²/sec or equivalent to 1.3×10^{16} H⁺/cm²/sec. With a yield of 0.034 SiO₂/H₃⁺ we have 1.5×10^{14} SiO₂ "molecules"/cm²/sec being removed. Thus only 1 in 10 of the incoming protons need react with a surface oxygen atom to balance the influx of diatomic atoms from the residual gases--even if it were pure oxygen at 2×10^{-6} torr. Since every incoming proton sooner or later diffuses from the lattice and generally does so via the surface at which it entered, it seems very probable that a few atomic layers of the bombarded surface are reduced to essentially pure metal. However, with a significant increase in the oxygen influx, this condition should not obtain.

How then do we understand that the H₃⁺ beam successfully drilled a hole in quartz (albeit with reduced yield), whereas the H₂⁺ beam had no visible effect? It should be noted that the respective H₂⁺ and H₃⁺ current densities are arranged to give nearly equal products of $j_1 Y_1$ so that the two holes, in general, emerge after nearly equal time delays. Apparently the reaction kinetics at or near the bombarded surface are different for H₂⁺ and H₃⁺. The average penetration depth for H₃⁺ will be less than that for H₂⁺ at the same energy per molecule. As a consequence, the concentrations of atomic hydrogen in the lattice and at its

surface will be different. Demonstration of this kinetic effect will be a subject of future research. The role of volatile hydrides must also be investigated.

IV. SPUTTERING YIELDS AT THE LUNAR SURFACE

The sputtering table which was presented in the First Quarterly Report is being revised in accordance with the latest information on solar wind and sputtering yield data.

A most important contribution came from the solar plasma experiments of the Mariner II. Preliminary data have been published for the period from 29 August to 31 October.⁸ The electrostatic spectrometer showed that a plasma flux from the direction of the sun was nearly always present at energies of 1664 and 2476 volts. This corresponds to proton velocities of 563 and 690 km/sec, respectively. Only occasionally did the energies become as low as 516 volts (314 km/sec) or as high as 8224 volts (1250 km/sec). In the 2-month period, 8 geomagnetic storms were detected. Analysis is given for one storm on 7 October 1962. The velocity of the ions kept increasing for approximately one day after the passage of the initial front. The plasma density increased by a factor of 5 and returned to its prestorm value about 5 hours after the storm front passed. Many of the spectra show two peaks. The lower voltage maximum could be due to protons and the higher due to α -particles. If the two species travel with approximately the same velocity away from the sun, the α -particles should appear at twice the voltage.

For quiet conditions, a plasma flux of $\sim 2 \times 10^8/\text{cm}^2 \cdot \text{sec}$ seems to be typical. The plasma velocity appears to be greater than that observed by Explorer X, and that predicted by Brandt and Michie⁹ and much higher than the values predicted by the solar breeze theories.¹⁰

Other pertinent information on the solar wind was published by Bader¹¹ who found with Explorer XII that the solar plasma stream loses its directional and supersonic characteristics at distances below 15 earth radii from the earth.

In the table which was presented in the First Quarterly Report, we assumed a flux of 10^9 protons/ $\text{cm}^2 \cdot \text{sec}$ with 250 km/sec. This number has now been changed to 2×10^8 protons/ $\text{cm}^2 \cdot \text{sec}$ with 600 km/sec. For solar storm conditions occurring on the average of twice per month and lasting 2×10^4 secs, we now estimate the flux increase to be only one order of magnitude greater than the quiescent value and we assume particle velocities of 1000 km/sec. We assume, as before, that 15% α -particles accompany the protons with the same velocities. We do not expect the sputtering yield of α -particles is any different from those of He^+ ions of the same velocity (km/sec). In an experiment, the only difference appears in the voltage-energy equivalent because α -particles would have to be accelerated to only half the voltage of the He^+ ions. We retain a factor of 2 for the more oblique incidence, a factor of 1/2 for the influence of the surface roughness (see Second Quarterly Report), and a factor of 1/2 for the fact that the lunar surface faces the sun only half the time.

Table II shows that the combined sputtering rate for Cu is $1.1 \text{ \AA}/\text{year}$ and for an average of various oxides of the order of $0.37 \text{ \AA}/\text{year}$. Thus, if one assumes that the solar wind remained unchanged over the period of the moon's existence, the moon must have lost in 4.5×10^9 years roughly a 17-cm-thick layer and in roughly 10^8 years a 1-cm-thick Cu plate would be sputtered away.

These results, of course, apply to meteorites as well. Micrometeorites especially must have a very limited lifetime (25,000 years for a 1-micron size particle!). Closer to the sun, the values increase with the inverse of the square of the distance to the sun. Thus, at the orbit of Mercury the values are 6.6 times higher than at the orbit of the earth.

Under such sputtering conditions, the surface of a space ship must eventually become atomically clean, which should simplify welding and soldering operations, but at the same time create problems with the increased friction of exposed sliding parts.

Heyman and Flint¹² recently took up the matter of meteorite sputtering and bombarded Fe as well as stone meteorite samples with Ar^+ ions. They found that, by volume, the sputtering rates of both kinds hardly differ. Their estimate of 0.05 atoms/ion for Fe under proton bombardment is, in our opinion, too high by a factor of 5.

V. THE LUNAR SURFACE STRUCTURE

An excellent, concise, survey article on surface properties of the moon was recently published by Öpik.¹³ Some fairly well established results described there can be summarized as follows:

The thermal conductivity of the surface layer is lower than any terrestrial substance and corresponds to mineral dust, in vacuo, of a grain size of about 0.1 mm. From the rate of cooling during an eclipse, one finds that a layer of greater conductivity is present at a depth of a few centimeters. The lunar dust is probably the result of battering by meteors, meteorites, and micrometeorites. Opik comes to the conclusion that most of the meteorite material vaporizes and escapes into space, while great amounts of loose lunar material are ejected and settle back as dust. The depth of penetration of the micrometeorites (dia. < 0.01 cm) into the dust layer is not expected to exceed 1 cm. The effects of meteorites, although much rarer in occurrence, may be comparable to those of the micrometeors although they penetrate deeper. The total mass of eroded dust is estimated to be 20 to 100 cm thick. The condensing vapors from the impact explosions may cause some cementation of the lunar dust. The accreted layer of micrometeor material in 4.5×10^9 years is estimated to be 20 cm, i.e., of the same order as that battered out from the surface rocks by the larger meteors. A complete turnover of the upper 1-centimeter layer by the action of micrometeorites would take place in about 10^4 years. In the radio wavelength range of 3 to 10 cm, the lunar surface behaves as a specular reflector with low reflectivity; this indicates that the average roughness is less than 10 cm. Three of the most remarkable features of the moon are the absence of limb darkening at full phase, the absence of any major color differences, and its low reflectivity.

Closer investigation of the photometric properties of the lunar surface¹⁴ reveals that ordinary terrestrial surfaces cannot reproduce the narrow lunar backscattering peak and the low albedo. A pelt of silver whiskers or very finely divided, dark, dielectric powders in a low state of compaction are about the closest approximation. Hapke¹⁴ concludes that the average size of the surface particles is between 1 and 50 microns, and that the entire lunar surface must be covered with such a layer at least several millimeters thick. Furthermore, the grains must be very opaque, much more so than terrestrial rocks.

Sytinskaya¹⁵ came to a similar conclusion and replaces the dust hypothesis in favor of a surface which resembles a spongy, sintered slag. Barabashov,¹⁶ who lists a number of other Russian references, concludes that the surface resembles honeycombed tuffs with extreme porosity and pittedness covered with pointed irregularities and parallel cracks. Fesenkov¹⁷ comes to similar conclusions and describes the structure as covered with deep holes with vertical walls and sharp edges and porous wells having a depth which is much greater than their width, resembling certain lichens.

Dust surfaces, which in our laboratory experiments were subjected to ion bombardment, show a remarkable correlation with the required lunar surface properties. Laboratory experiments have the advantage that one can perform the bombardment with much higher flux densities and simulate the solar wind effects in a much shorter time. In our Hg^+ -ion experiments (which do not, of course, simulate possible additional chemical reactions

between hydrogen and the target material) with current densities of 5 ma/cm^2 , and sputtering yields of 1 atom/ion, we accelerate the lunar H^+ -ion bombardment and sputtering conditions by a factor of 1.5×10^8 in flux and ~ 100 in sputtering yield. One hour of our laboratory sputtering is equivalent to $\sim 1.5 \times 10^{10}$ hours or 2×10^6 years of sputtering at the moon's surface.

As partly described in the First Quarterly Report, we can summarize our findings on ion-bombarded, oxide dust surfaces (such as Al_2O_3 , CuO , Cu_2O , FeO , and Fe_2O_3) as follows:

1. The surface becomes covered with a crust with dust particles cemented together by sputtered atoms.
2. The surface layer becomes enriched with metal atoms. In the process of breaking up molecules, and sputtering atoms back and forth, oxygen atoms are more likely to escape than metal atoms. This process of metal enrichment is probably further enhanced by chemical reactions with the hydrogen ions.
3. We can, furthermore, assume that heavy metal atoms are favored for being retained while the light, sputtered atoms have a high probability for escaping from the moon. Therefore, we would predict an enrichment with heavy metals at the lunar surface.
4. The surface crust has a structure which is strikingly similar to that required from lunar photometric observations, i.e., a fibrous surface with closely spaced needles and spires, and deep small holes with a slag-like, opaque appearance. The predominance of microscopically very steep walls is evidenced by the fact that the surface looks rather dark when

illuminated and viewed perpendicular to the macroscopic surface, but becomes very bright when illuminated and viewed from the same oblique direction. Bombardment in these experiments was always under normal incidence (to the macroscopic surface) and the needles and holes in these samples all point in directions normal to the surface. At the moon this is not the case, and the bombardment sweeps the surface over a range of angles from minus to plus 90° in the equatorial plane. This should cause the surface to become irregular and more complex, but will not change its basic character.

Hapke¹⁴ has recently performed some interesting studies with 10-keV proton bombardment of minerals. With $20 \mu\text{a}/\text{cm}^2$ ion current density, he bombarded targets of Ag_2S , Fe_2O_3 , Al_2O_3 , SiO_2 , MgO , etc., for a period of one week (about 10 coulombs) and finds whisker growth at the Ag_2S powder sample, reduction of the red Fe_2O_3 powder to black Fe_3O_4 or FeO , and coating of the Al_2O_3 with powder grains with a dark metallic layer (probably Al). With compact solid rather than powder samples, sintered alumina had only a slight yellowish tint, and quartz had no discoloration at all. More or less, these results substantiate our observations. The puzzling part of these experiments is the fact that cementing together of dust particles was never observed and that the bombarded powder targets show a loss of material which exceeds anything which can be explained by physical sputtering. With 10 coulombs of 10 keV H^+ ions we would predict a thickness reduction which is more in the micron than in the millimeter range observed by Hapke. We suspect that the (non-mass-separated) beam in Hapke's

experiments contained a substantial number of heavier ions and charge-exchange neutrals which are responsible for the major part of the sputtering; or else, chemical reactions have a much more pronounced influence on sputtering yields than anticipated; or that dust particles were lost by electrostatic charging effects. With respect to our observed cementing of particles, we can certainly discard the joule heating of contact points as a possible reason. We think that the difference between Hapke's and our results is more likely to be found in our much higher sputtering rates since we bombard the target with several hundred coulombs and with ions which are $\sim 10^2$ times more efficient in sputtering.

TABLE I

Z	Metal	$D(\frac{\text{mg}}{\text{cm}^2})$	kv	$10^3 Y_2$	$10^3 \Delta Y_2$	$10^3 Y_3$	$10^3 \Delta Y_3$	$R = Y_3 / Y_2$	ΔR	Comments
4	Be	3.86	7.2	32.0	1.0	46.0	1.5	1.44	.06	
13	Al	10.5	6.9	27.0	1.0	42.0	1.5	1.45	.06	
22	Ti	26.0	7.0	10.9	0.3	15.3	0.5	1.40	.06	I_T shift meg.
23	V	28.2	8.0			16.5	0.6			
26	Fe	19.2	7.2	18.1	0.9	26.5	1.3	1.46	.08	
			7.5	23.8	0.5	30.2	0.7	1.27	.04	
27	Co	26.4	8.0	17.0	0.7	22.1	0.7	1.30	.06	10% shift in I_T
28	Ni	23.4	7.8	35.2	1.1	52.3	1.6	1.49	.06	
			7.2	37.0	2.0	58.0	3.0	1.57	.11	
			7.5	35.5	1.1	58.5	1.8	1.63	.07	
29	Cu	48.9	7.5	37.7	1.1	61.1	1.8			
			5.9	76.0	4.0	115.0	6.0	1.51	.11	
			6.0			112.0	5.0			
			7.2	61.6	1.2	89.6	1.8	1.46	.04	
			8.7	59.5	1.8	93.6	3.0	1.57	.07	
40	Zr	36.9	9.7	57.4	1.4	100.9	2.5	1.76	.06	
			7.2	7.6	0.2	10.3	0.5	1.35	.08	
42	Mo	26.1	7.5	6.8	0.2	9.6	0.3	1.41	.06	5% shift in I_T
46	Pd	32.4	6.9	11.2	0.2	11.1	0.2	0.99	.03	
47	Ag	26.1	7.5	23.6	0.7	38.0	1.2	6.61	.07	
			5.0	61.0	1.2	92.0	1.8	1.51	.05	
			6.3	56.0	1.2	85.0	1.8	1.52	.05	
73	Ta	28.7	6.9	53.0	1.2	88.0	1.8	1.66	.05	
74	W	54.0	6.3	3.0	0.06	2.22	0.09	0.74	.03	
75	Re	84.7	8.0	1.61	0.08	1.93	0.10	1.20	.08	10% shift in I_T
77	Ir	65.5	6.8	5.77	0.13	7.22	0.16	1.25	.04	
78	Pt	55.7	7.5	14.1	0.7	11.9	0.6	0.77	.05	10% shift in I_T
79	Au	52.2	7.5	12.3	0.4	16.9	0.5	1.37	.06	
			7.0	33.5	1.2	35.4	1.2	1.06	.04	Questionable foil
13	Al*	49.3	8.0	36.0	1.1	56.5	1.7	1.57	.07	New foil
73	Ta*		6.9	22.4	0.6	34.8	1.0	1.55	.07	39 μ thick
			6.7	2.96	0.06	2.65	0.08	0.89	.04	17 μ thick

* Anodized to oxide 0.30 μ thick on each surface.

TABLE II

<u>Ion</u>	<u>Flux</u>	<u>Velocity</u>	<u>Energy</u>	Yield (atoms/ion) (Normal incidence, smooth surface)	<u>Sputtering Rate at Moon</u>	
					Atoms/cm ² .Year	$\frac{\text{Å}}{\text{Year}}$
Proton (solar wind)	$2 \times 10^8/\text{cm}^2 \cdot \text{sec}$	600 km/sec	1850 ev	Cu: 0.03 Fe: 0.009 Oxides: 0.01	0.1×10^{15} 0.03×10^{15} 0.03×10^{15}	0.3 0.1 0.1
Proton (solar storm)	$2 \times 10^9/\text{cm}^2 \cdot \text{sec}$ for 1/60 of time	1000 km/sec	5 kev	Cu: 0.04 Fe: 0.008 Oxides: 0.009	0.02×10^{15} 0.004×10^{15} 0.004×10^{15}	0.06 0.012 0.012
α -particle (solar wind)	$0.3 \times 10^8/\text{cm}^2 \cdot \text{sec}$	600 km/sec	3700 ev equivalent to He ⁺ ion at 7400 ev	Cu: 0.5 Fe: 0.15 Oxides: 0.16	0.23×10^{15} 0.07×10^{15} 0.08×10^{15}	0.7 0.21 0.24
α -particle (solar storm)	$3 \times 10^8/\text{cm}^2 \cdot \text{sec}$ for 1/60 of time	1000 km/sec	10 kev equivalent to He ⁺ ion at 20 kev	Cu: 0.2 Fe: 0.06 Oxides: 0.07	0.015×10^{15} 0.005×10^{15} 0.006×10^{15}	0.045 0.015 0.018

3269

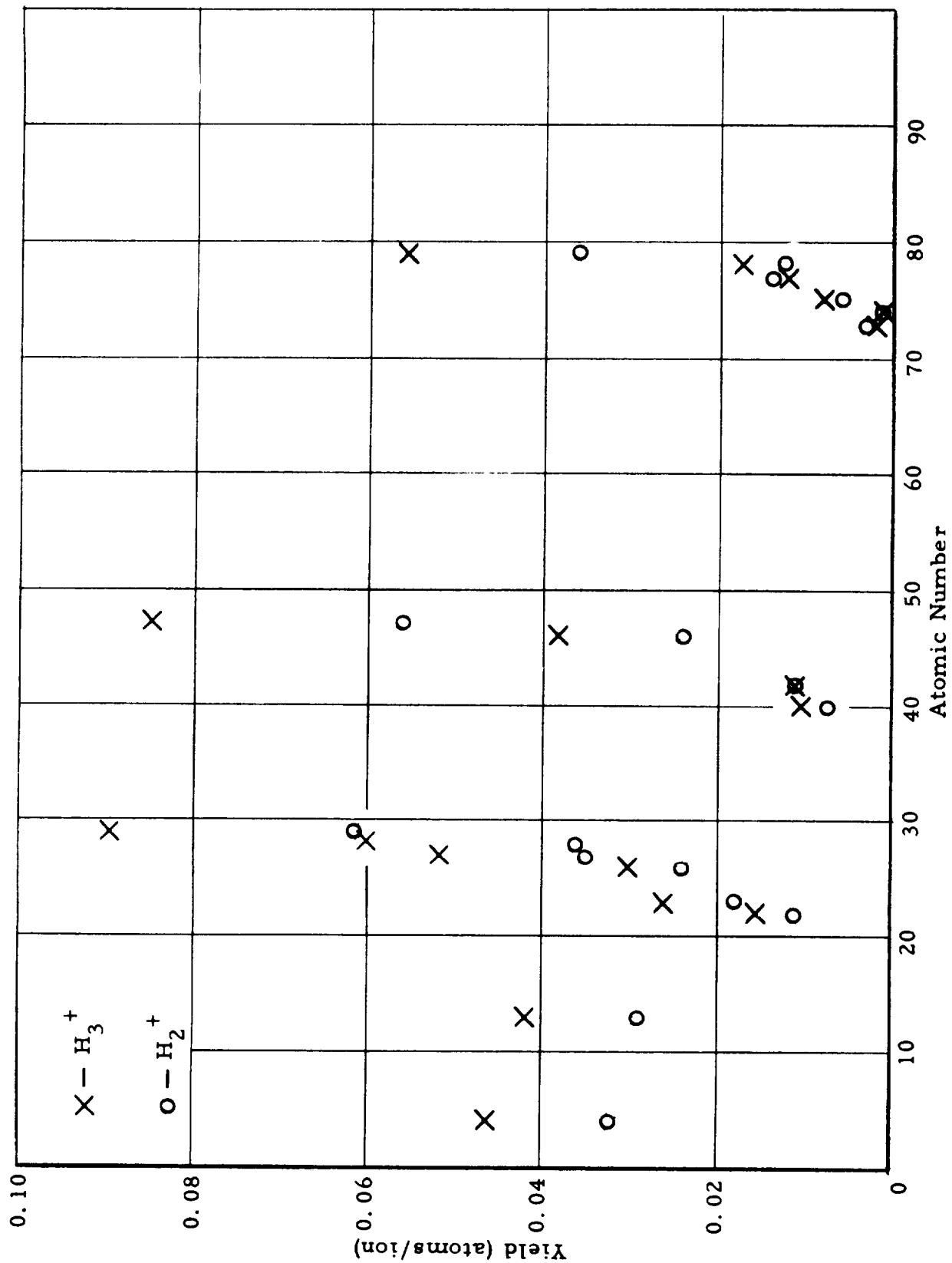


Fig. 1 Sputtering Yields for H_2^+ and H_3^+ Ions at 7 keV as a Function of Atomic Number

VI. PERSONNEL

The following personnel under the guidance of Dr. G. K. Wehner contributed to this work: D. L. Rosenberg (sputtering of rocks and powders in a Hg plasma, literature survey), C. E. KenKnight (mass separated hydrogen beam studies), T. Stafford (technician), and E. Benz and A. Haut (glass experts).

VII. REFERENCES

1. O'Briain, C. D., A. Lindner and W. J. Moore. Sputtering of silver by hydrogen ions. *J. Chem. Phys.* 29: 3-7 (1958).
2. Grönlund, F. and W. J. Moore. Sputtering of silver by light ions with energies from 2 to 12 kev. *J. Chem. Phys.* 32: 1540-45 (1960).
3. Yonts, O. C., C. E. Normand and D. E. Harrison. High-energy sputtering. *J. Appl. Phys.* 31: 447-50 (1960).
4. General Mills, Inc. Electronics Div. Report no. 2354. Surface bombardment studies, by G. K. Wehner, G. S. Anderson and C. E. KenKnight. Contract AT(11-1)-722. Technical Progress Report (Nov. 15, 1962).
5. Wehner, G. K. and D. Rosenberg. Mercury ion beam sputtering of metals at energies 4-15 kev. *J. Appl. Phys.* 32: 887-90 (1961).
6. Wolsky, S. P. and E. J. Zdanuk. Investigation of the sputtering of silicon. *J. Appl. Phys.* 32: 782-86 (1961).
7. Yonts, O. C. and D. E. Harrison. Surface cleaning by cathode sputtering. *J. Appl. Phys.* 31: 1583-84 (1960).
8. Neugebauer, M. and C. W. Snyder. Solar plasma experiment. *Science* 138: 1095-96 (1962).
9. Brandt, J. C. and R. W. Michie. Interplanetary gas. VII. A semi-empirical model. *Astrophys. J.* 136: 1023-31 (1962).
10. Chamberlain, J. W. Interplanetary gas. II. Expansion of a model solar corona; III. A hydrodynamic model of the corona. *J. Geophys. Res.* 131: 47-56 (1960); 133: 675-87 (1961).
11. Bader, M. Preliminary Explorer 12 data on protons below 20 kev. *J. Geophys. Res.* 67: 5007-11 (1962).
12. Heymann, D. and J. M. Fluit. Sputtering by 20-kev Ar^+ ions at normal incidence on meteorites. *J. Geophys. Res.* 67: 2921-24 (1962).
13. Opik, E. J. Surface properties of the moon. *In Progress in the Astronautical Sciences*, vol. 1. Amsterdam, North-Holland Publ. Co., 1962. pp. 219-60.
14. Cornell University Center for Radiophysics and Space Research. Report 127. Experiments relating to the lunar surface. I. Photometric studies. II. Proton bombardment of minerals, by B. W. Hapke (July 1, 1962).

VII. REFERENCES (Continued)

15. Sytinskaya, N. N. New data on the meteoric-slag theory of the formation of the outer layer of the lunar surface. *Astron. Zh.* 36: 315-21 (1959).
16. Barabashov, N. P. The structure of the moon's surface and a study of the first photographs of its reverse side. *Planetary Space Sci.* 9: 835-40 (1962).
17. Fessenkov, V. G. Photometry of the moon. In *Physics and Astronomy of the Moon*, ed. by Z. Kopal. N.Y., Academic Press, 1962. pp. 99-130.